

7. Birge, R. R. *et al.* Protein based associative processors and volumetric memories. *J. Phys. Chem. B*, 1999, **103**, 10746–10766.
8. Hampp, N., Thoma, R., Zeisel, D. and Brauchle, C., Bacteriorhodopsin variants for holographic pattern recognition in molecular and biomolecular electronics. *Adv. Chem.*, 1994, **240**, 511–526.
9. Downie, J. D. and Smithey, D. T., Measurement of holographic properties of bacteriorhodopsin films. *Appl. Opt.*, 1996, **35**, 5780–5789.
10. Huang, J. Y., Chen, Z. and Lewis, A., Second-harmonic generation in purple membrane-poly(vinyl alcohol) films: probing the dipolar characteristics of the bacteriorhodopsin chromophore in bR570 and M412. *J. Phys. Chem.*, 1989, **93**, 3314–3320.
11. Reddy, K. P. J., Passive mode locking of lasers using bacteriorhodopsin molecules. *Appl. Phys. Lett.*, 1994, **64**, 2776–2778.
12. Reddy, K. P. J., Analysis of light-induced processes in bacteriorhodopsin and its application for spatial light modulation. *J. Appl. Phys.*, 1995, **77**, 6108–6113.
13. Ippen, E. P., Shank, C. V. and Dienes, A., Rapid photobleaching of organic laser dyes in continuously operated devices. *IEEE J. Quantum Electron.*, 1971, **QE-7**, 178–179.
14. Moller, C., Buldt, G., Dencher, N. A., Engel, A. and Muller, D. J., Reversible loss of crystallinity on photobleaching purple membrane in the presence of hydroxylamine. *J. Mol. Biol.*, 2000, **301**, 869–879.
15. Dubois, A., Canva, M., Brun, A., Chauput, F. and Boilot, J. P., Photostability of dye molecules trapped in solid matrices. *Appl. Opt.*, 1996, **35**, 3193–3199.
16. Dubois, A., Canva, M., Brun, A., Chauput, F. and Boilot, J. P., Enhanced photostability of dye molecules trapped in solid xerogel matrices. *Synth. Metals*, 1996, **81**, 305–308.
17. Sukhdev Roy and Reddy, K. P. J., Modelling of light modulation processes in D85N bacteriorhodopsin. *Curr. Sci.*, 2000, **78**, 184–188.
18. Sukhdev Roy, Singh, C. P. and Reddy, K. P. J., Generalized model of all-optical light modulation in bacteriorhodopsin. *J. Appl. Phys.*, 2001, **90**, 3679–3688.

ACKNOWLEDGEMENT. This work was performed while K.P.J.R. was at Nee Ann Polytechnic as a consultant.

Received 3 June 2003; revised accepted 10 October 2003

Synoptic hydrology of India from the data of isotopes in precipitation

S. K. Gupta* and R. D. Deshpande

Physical Research Laboratory, Navrangpura, Ahmedabad 380 009, India

Recently, regional maps of amount weighted monthly isotopic data of precipitation have become available from the GNIP/IAEA database (<http://isohis.iaea.org>). These maps are based on stations for which at least one complete year of isotopic and precipitation data were available. In this communication an attempt has been made to discern and describe the hydrological processes responsible for giving characteristic regio-

nal distribution of $\delta^{18}\text{O}$ and '*d*-excess' for different seasons over the Indian subcontinent. It is shown that the characteristic isotopic signal is imparted to precipitation initially by the two primary oceanic sources of vapour influx, namely the Arabian Sea and the Bay of Bengal during both the summer and winter monsoon seasons. Subsequently, the processes of evaporation and transpiration redistribute and recycle the water between the atmosphere and the land surface. The isotopic data help in identifying the geographical regions where any source/process dominantly influences the precipitation signal.

PRECIPITATION is of major interest in the hydrologic cycle as it is the primary source of water on land. Therefore, an understanding of the formation of precipitation and its variations are important to a hydrologist. Similarly, understanding the processes controlling temporal and geographic variations of isotopic composition of precipitation is equally important to an isotope hydrologist. The meteoric processes modify the isotopic composition of water in such a way that precipitation in a particular environment has a characteristic isotopic signature. This signature then serves as a natural tracer for the provenance of groundwater. Characterizing the stable isotope distribution in meteoric waters is, therefore, essential in determining the input function for most isotopic hydrology applications.

Realizing the importance of the basic data on isotopic composition of precipitation to hydrology, the International Atomic Energy Agency (IAEA), in collaboration with World Meteorological Organization (WMO) established the Global Network of Isotopes in Precipitation (GNIP) at which samples are collected to monitor the $\delta^{18}\text{O}$ and δD of precipitation. The data produced by this network are available on the World Wide Web at <http://isohis.iaea.org>.

In the Indian context, the Arabian Sea (AS)¹ and the Bay of Bengal (BOB) are the two oceanic moisture sources that primarily feed the rainfall during two seasons, namely southwest summer monsoon (June–September) and northeast winter monsoon (October–January, refs 2 and 3; C. K. Rajan, unpublished). In addition, locally recycled vapour from within and around India as also long-distance transport of vapour under the influence of western disturbances contribute to rainfall². These vapour sources are expected to have characteristic isotopic signatures. Further, evaporation from falling raindrops under the conditions of low humidity and high temperature in parts of the country during certain periods can impart distinctive isotopic signatures to rainfall. The isotopic composition of precipitation can therefore be used to discern the influence of different vapour sources and post-precipitation processes. In the following, starting with some relevant basic concepts, an attempt is made to describe the hydrological processes responsible for giving characteristic regional distribution of $\delta^{18}\text{O}$ and '*d*-excess' for different seasons over the Indian subcontinent.

*For correspondence. (e-mail: skgupta@prl.ernet.in)

Stable isotope compositions of oxygen and hydrogen are normally reported as δ values in units of parts per thousand (denoted as ‰; permil) relative to a standard of known composition. The δ values are calculated by

$$\delta (\text{in } \text{‰}) = (R_x/R_s - 1)1000, \quad (1)$$

where R denotes the ratio of heavy to light isotope (e.g. $^{18}\text{O}/^{16}\text{O}$ or D/H) and R_x and R_s are the ratios in the sample and standard respectively. δD and $\delta^{18}\text{O}$ values are normally reported relative to SMOW (Standard Mean Ocean Water⁴) or the equivalent VSMOW (Vienna-SMOW) standard⁵.

Two main types of phenomena produce isotopic fractionations: equilibrium isotopic exchange reactions and kinetic processes. Equilibrium isotope exchange reactions involve the redistribution of isotopes between the products and reactants (or the two phases during phase change) as they remain in contact with each other. In systems out of equilibrium, reaction products are isolated from the reactants and isotope reactions may, in fact, be unidirectional. Such reactions are called kinetic reactions.

It has been shown that in spite of the great complexity in different components of the hydrological cycle, $\delta^{18}\text{O}$ and δD in freshwater correlates on a global scale⁶ in the form of an empirical relation known as Global Meteoric Water Line (GMWL)⁷.

$$\delta\text{D} = 8.\delta^{18}\text{O} + 10 (\text{‰ SMOW}). \quad (2)$$

GMWL indicates that the isotopic composition of meteoric waters behaves in a predictable manner. The line is, of course, global in application, and is actually the average of many local or regional meteoric water lines, which differ from the global line due to varying climatic and geographic parameters. The slope 8 of GMWL is due to the ratio (8.2 at 25°C) of isotopic fraction factors of ^2H and ^{18}O during condensation, which is largely an equilibrium process. The intercept 10 is due to kinetic fractionation during evaporation of ocean water (at ~85% humidity)⁷.

The evolution of $\delta^{18}\text{O}$ and δD composition of meteoric waters begins with evaporation from the oceans, where the rate of evaporation limits vapour–water exchange and so limits the degree of isotopic equilibrium. Increased rates of evaporation impart a kinetic or non-equilibrium isotope effect on the vapour. Kinetic effects are influenced by surface temperature, wind speed (shear at water surface), salinity and most importantly, humidity. At lower humidity, water–vapour exchange across the boundary layer becomes increasingly unidirectional (water to air), and evaporation becomes increasingly a non-equilibrium process.

Gonfiantini⁸ describes the isotopic enrichment ($\Delta\epsilon$) at humidity (h) due to kinetic fractionation by the following two relationships:

$$\Delta\epsilon^{18}\text{O}_{\text{bl-v}} = 14.2(1 - h)\text{‰}, \quad (3)$$

$$\Delta\epsilon^2\text{H}_{\text{bl-v}} = 12.5(1 - h)\text{‰}, \quad (4)$$

where the symbol $\Delta\epsilon_{\text{bl-v}}$ represents isotopic enrichment during vapour formation across a thin boundary layer. The total enrichment between water column and open air is the sum of the enrichment factor for equilibrium water vapour exchange ($\epsilon_{\text{l-v}}$) and the kinetic factor ($\Delta\epsilon_{\text{bl-v}}$). For ^{18}O , this would be

$$\delta^{18}\text{O}_\text{l} - \delta^{18}\text{O}_\text{v} = \epsilon^{18}\text{O}_{\text{l-v}} + \Delta\epsilon^{18}\text{O}_{\text{bl-v}} \quad (5)$$

Under conditions of 100% humidity ($h = 1$), the vapour is in isotopic equilibrium with sea water ($\Delta\epsilon^{18}\text{O}_{\text{bl-v}} = 0$). When humidity is low (e.g. $h = 0.5$), the vapour is strongly depleted in heavy isotopes, relatively more in case of ^{18}O compared to D (eqs (3) and (4)). The evolution of an evaporating water body on a $\delta^{18}\text{O}$ – δD plot, therefore, follows a path with a slope < 8 , depending on the humidity.

If a parameter ‘ d ’ = ‘ d -excess’ = $\delta\text{D} - 8.\delta^{18}\text{O}$ (‰) is defined⁹, it can be seen that the ‘ d -excess’ of the evaporating water body will progressively decrease and that of the resulting vapour will progressively increase. Therefore, ‘ d -excess’ provides a handle⁸ on identifying waters and vapours that have undergone kinetic evaporation under humidity $< 100\%$. The global atmospheric vapour forms with an average humidity around 85% ($h = 0.85$), imparting a deuterium intercept of 10‰ to GMWL⁹.

If the original water was meteoric in origin (i.e. with ‘ d -excess’ ~10‰), the residual water will be enriched in heavy isotopes but will be showed progressively lower ‘ d -excess’ values as the evaporation proceeds. The resulting vapour will show the opposite effect. This, however, is not the case with transpiration as it returns essentially un-fractionated water to the atmosphere¹⁰, despite the complex fractionation in leaf water^{10,11}. Thus, transpiration cancels out the effect of rainout process. On the other hand, evaporated vapour is usually depleted in heavy species relative to that of transpired vapour and is actually closer to the composition of the atmospheric vapour.

Further partitioning of ^{18}O and D between different regions is caused during rainout by Rayleigh distillation process⁶. Along the trajectory of the air masses, each rainout distills the heavy isotopes from the vapour. Therefore, in the rainout process, not only does the vapour mass decrease progressively, but the remaining vapour also becomes progressively depleted in ^{18}O and D . One can model this isotope evolution during rainout according to Rayleigh distillation equation⁷ as below:

$$R = R_0 f^{(\alpha-1)} \quad (6)$$

In this case, R_0 is the initial isotope ratio ($^{18}\text{O}/^{16}\text{O}$ or D/H) of the precipitating vapour and R represents the iso-

tope ratio after a given proportion of the vapour has rained out. The residual vapour reservoir fraction is denoted by f and α denotes the equilibrium water–vapour fractionation factor at the prevailing ‘in cloud’ temperature. The rainout process, therefore, does not modify the ‘ d -excess’ of the precipitating vapour.

With the above background, it is now possible to interpret the observed seasonal changes in $\delta^{18}\text{O}$ and ‘ d -excess’ of rainwater from the Indian region as depicted in Figures 1 and 2 respectively. Both the figures have been downloaded and appropriately cropped from the monthly regional data available at <http://isohis.iaea.org>. They show seasonal variations in $\delta^{18}\text{O}$ and ‘ d -excess’ in precipitation from India and the neighbouring stations for the four selected months. In spite of the limited data of isotopes in precipitation and the knowledge that these figures provide only a broad generalized picture, some salient points emerge.

Starting with the month of August, in the middle of the SW monsoon season, a progressive decrease in $\delta^{18}\text{O}$ is seen from $> -2\text{‰}$ on the Western Ghats to $< -10\text{‰}$ in the

foothills of Nepal Himalayas along the SW to NE direction (Figure 1*b*), indicating vapour source from the Arabian Sea. It is important to note that $\delta^{18}\text{O}$ values $> -2\text{‰}$ are confined to the region of the Western Ghats where, due to orographic uplift, the vapour-laden SW monsoon current from the AS causes heavy rains. In the rain-shadow region of the Western Ghats and farther east and north, the $\delta^{18}\text{O}$ values in precipitation appear to decrease due to rainout. During August, the ‘ d -excess’ on the other hand, varies between 8 and 12‰ on the western coast and in NNE along the foothills of Himalayas and the Gangetic plains (Figure 2*b*). These two regions with $\sim 10\text{‰}$ ‘ d -excess’ are separated by a region of lower ‘ d -excess’ ($< 8\text{‰}$) covering the southern part of the east coast, central India and parts of western India (Figure 2*b*). In this region of low ‘ d -excess’, precipitation during the SW monsoon is $< 50\text{ cm}$ (ref. 12). Consequently, relative humidity is low and temperatures relatively high. In part, the region of $< 8\text{‰}$ ‘ d -excess’ overlies the rain-shadow region of the Western Ghats. It is likely that evaporation from falling raindrops is responsible for

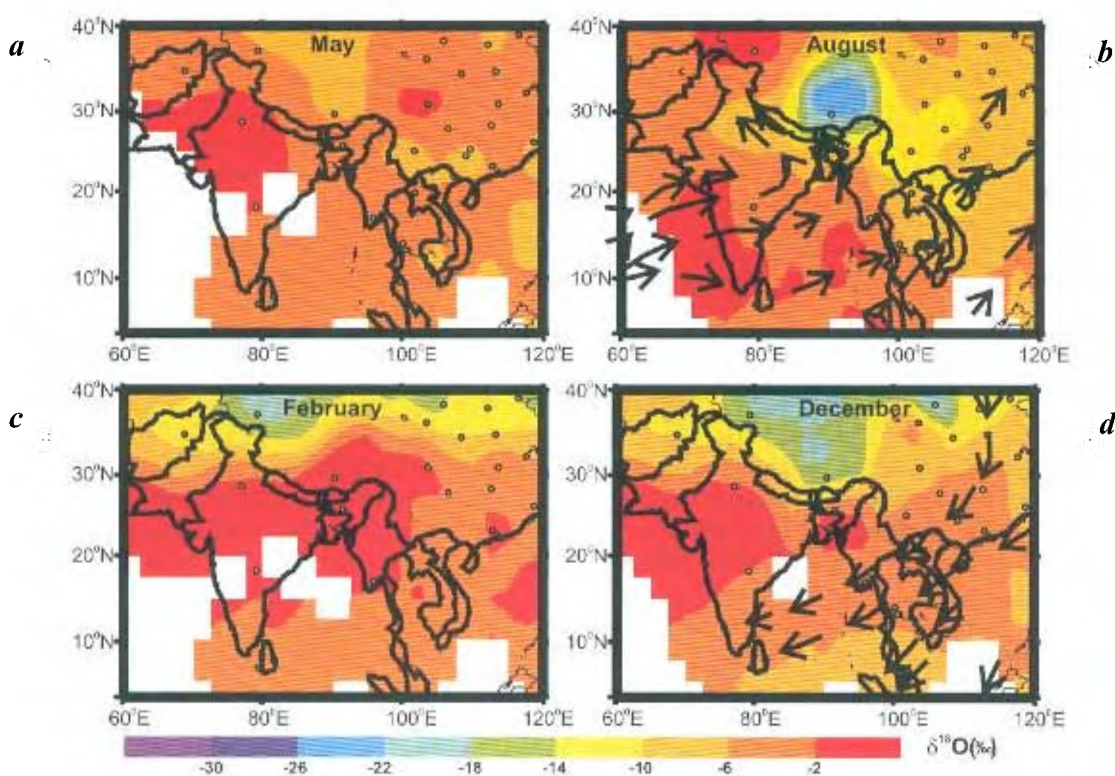


Figure 1 a–d. Maps showing distribution of amount-weighted $\delta^{18}\text{O}$ in monthly precipitation for May, August, December and February downloaded and appropriately cropped from the monthly regional data available at <http://isohis.iaea.org>. Open circles represent the locations of the GNIP/IAEA network of stations for which at least one full year of data were available and have been used in the preparation of these maps. The SW summer monsoon and the NE winter monsoon circulations (redrawn from ref. 2) are superposed over the maps for August and December, respectively.

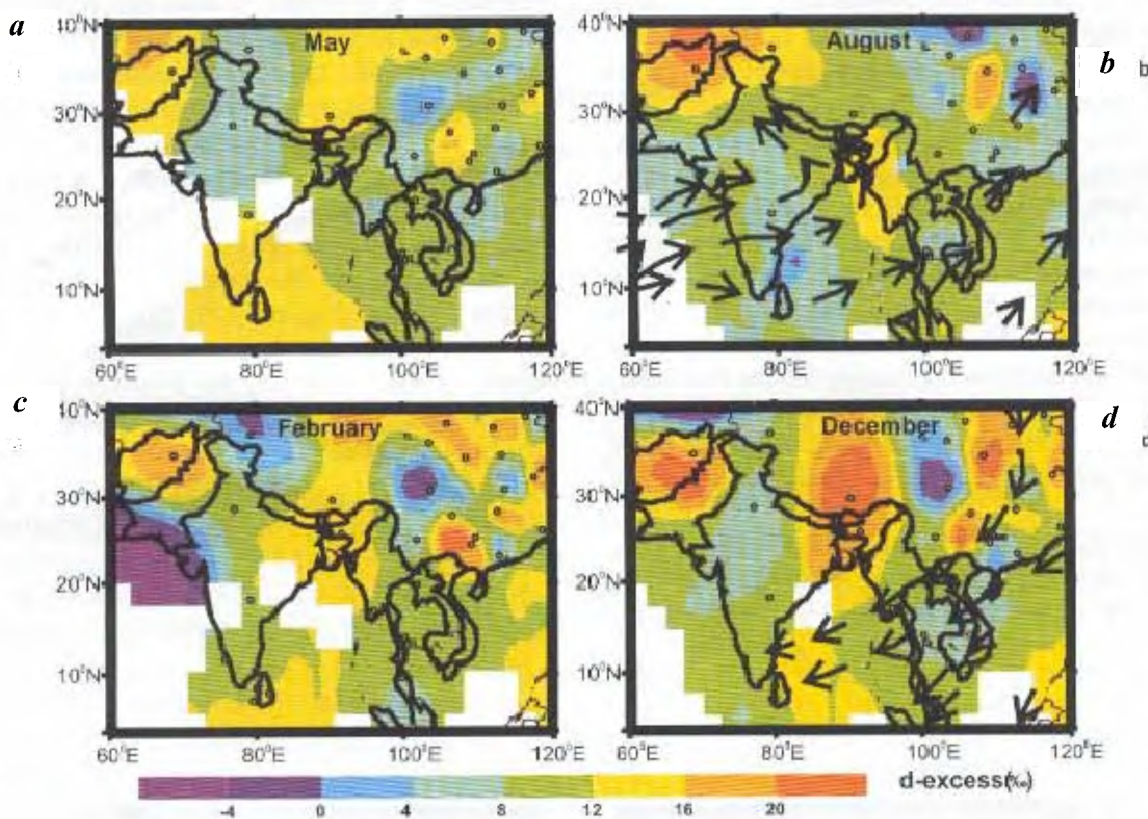


Figure 2 a–d. Same as Figure 1, but for the parameter ‘*d*-excess’.

lower values of ‘*d*-excess’ (<8‰) in precipitation in this region. Just as the ‘*d*-excess’ values in the range 8–12‰ in precipitation along the west coast are indicative of the unmodified oceanic vapour source from the AS/Indian Ocean, similar values in NNE along the foothills of the Himalayas and Gangetic Plains are due to significant addition of oceanic vapour from the BOB to the rejuvenated monsoon current as it turns anticlockwise to re-enter India over the northern part of the east coast, in the form of the BOB branch of the Indian summer monsoon. Interestingly, the region over Bangladesh and the eastern states of Tripura, Manipur and eastern Myanmar show ‘*d*-excess’ values in precipitation >12‰. This is likely to arise by recycling of precipitated water by evaporation from the large area of wetlands in the region during this season.

Moving to the month of December in the middle of the NE winter monsoon, it is noticed that the $\delta^{18}\text{O}$ of the precipitation over wetlands in Bangladesh and eastern India has changed from <–6‰ in August to >–2‰ in December (Figure 1d) and is accompanied by even higher (16–20‰) values of ‘*d*-excess’ (Figure 2d), indicating that during winters, small amount of precipitation that occurs in this region derives a significant component of vapour by evaporation from local sources. During the same period

the $\delta^{18}\text{O}$ values in southern India and Sri Lanka decrease from >–2‰ (Figure 1d), indicating vapour source from the isotopically light surface water of BOB, further confirmed by the ‘*d*-excess’ in the 8–12‰ range (Figure 2d). The >–2‰ $\delta^{18}\text{O}$ values in central and western India and also northern parts of the west coast region (Figure 1d) may be indicative of vapour source in the AS but with significant evaporation from the falling raindrops, as indicated by lower (4–8‰) ‘*d*-excess’ values (Figure 2d). Because of the rainy season in southern India during winter and the largely oceanic vapour source, the region of low (<8‰ *d*-excess) seen in August in this part shifts to the northern and western parts of the country.

In the month of February, only scattered rain is recorded in the country in southern India and parts of North India (Jammu and Kashmir, Punjab, Haryana, western Uttar Pradesh, under the influence of western disturbances). Both $\delta^{18}\text{O}$ and ‘*d*-excess’ show (Figures 1c and 2c) a pattern similar to December in southern India, albeit with reduced area. The region of high $\delta^{18}\text{O}$ values (>–2‰) now covers the entire central part of India from west to east (Figure 1c). It is not possible to ascertain if this is an indication of vapour source in the AS or recycling of evaporated vapour of land origin. Possibly, both these

factors are operative but with a significant contribution from land-derived recycling. The region of high '*d*-excess' (>12‰) over Bangladesh and eastern India spreads westwards (Figure 2c), indicating precipitation from largely evaporative recycled vapour. Extremely low values of '*d*-excess' (<4 to <0‰) are seen in precipitation over Gujarat, clearly indicating high evaporation from raindrops during occasional rains during this season. The region of '*d*-excess' ~10‰ in the central and northern parts of India (Figure 2c) during this season cannot be explained as due to precipitation of primary oceanic vapour, but is an equilibrium value due to evaporation from falling raindrops with recycled vapour either from Afghanistan and west Pakistan, or from the eastern parts (Bihar, West Bengal and other eastern states of India) or of local origin. This interpretation is favoured because both rainfall and relative humidity in much of India are low during this season.

The month of May is the driest month of the year. The $\delta^{18}\text{O}$ values in precipitation (Figure 1a) are high (>-2‰) in central and western India and about the same (-6 to -2‰) as in December and February in southern India. The lowering of $\delta^{18}\text{O}$ values from >-2‰ in February to <-2‰ in May, seen in eastern India and Bangladesh, is indicative of fresh vapour influx from the northern BOB. This is also indicated by a decrease in '*d*-excess' value of precipitation (Figure 2a) from the previous season (from >12 to ~10‰). The dry conditions continue to prevail over central and northwest India indicated by '*d*-excess' of <8‰. Over southern India and Sri Lanka, the '*d*-excess' values of precipitation increase from ~10‰ in February to >12‰, indicating local recycling of vapour. Alternatively, this could also indicate marine vapour source from the southern BOB evaporating under low (<85%) relative humidity.

To summarize, primary oceanic vapour influx areas along the west and east coasts both during SW summer and NE winter monsoons are characterized by '*d*-excess' in the range 8–12‰. Due to continued aridity even during the period of summer monsoons, the rain-shadow zone of the Western Ghats, parts of the southeast coast, central and northwest India, show clear indication of evaporation from falling raindrop in the form a belt of low (<8‰) '*d*-excess' values. The region over Bangladesh and the eastern states of Tripura, Manipur and eastern Myanmar show high (>12‰) '*d*-excess' values in precipitation for most of the year, except at the beginning of May. From August onwards, the area covered by this high '*d*-excess' region progressively increases and spreads westwards, indicating evaporative recycling of vapour from large area of wetlands and soil moisture during the monsoon and post-monsoon seasons. Another region of persistent recycled vapour of land origin lies over Afghanistan and Pakistan. It spreads to Jammu and Kashmir during winter–spring under the influence of western disturbances, as seen clearly in the low $\delta^{18}\text{O}$ (-14 to -6‰) values of pre-

cipitation. This spread of land-derived vapour during winter–spring is not so clearly seen in enhanced '*d*-excess' values over Jammu and Kashmir as evaporation from the falling raindrops reduces their high '*d*-excess' values, to ~10‰. The lowering of $\delta^{18}\text{O}$ values in May, seen in eastern India and Bangladesh, indicate the onset of vapour influx from the northern BOB. This is also indicated by a decrease in '*d*-excess' value of precipitation from the previous season (from >12 to ~10‰).

It is thus seen that even with limited availability of data of isotopes in precipitation, it is possible to postulate on a regional scale, vapour fluxes and hydrological processes. These interpretations can be sharpened and reasonably good quantitative estimates can be made, if systematically monitored data from bigger networks on both precipitation and vapour could be collected.

1. Ghosh, S. K., Pant, M. C. and Dewan, B. N., Influence of Arabian Sea on the Indian summer monsoon. *Tellus*, 1978, **30**, 117–125.
2. Das, P. K., *The Monsoons*, National Book Trust, India, 1995, p. 252.
3. Rao, Y. P., South west monsoon. *Meteorological Monograph, Synoptic Meteorology*, India Meteorological Department, 1976, p. 367.
4. Craig, H., Standards for reporting concentrations of deuterium and oxygen-18 in natural water. *Science*, 1961, **133**, 1833–1834.
5. Gonfiantini, R., Standards for stable isotope measurements in natural compounds. *Nature*, 1978, **271**, 534–536.
6. Craig, H., Isotopic variations in meteoric waters. *Science*, 1961, **133**, 1702–1703.
7. Clark, I. and Fritz, P., *Environmental Isotopes in Hydrogeology*, Lewis Publishers, Boca Raton, 1997, p. 328.
8. Gonfiantini, R., Environmental isotopes in lake studies. In *Handbook of Environmental Isotope Geochemistry: The Terrestrial Environment* (eds Fritz, P. and Fontes, J.-Ch.), Elsevier, Amsterdam, The Netherlands, 1986, vol. 2, pp. 113–168.
9. Dansgaard, W., Stable isotopes in precipitation. *Tellus*, 1964, **16**, 436–438.
10. Zimmermann, U., Munnich, K. O. and Roether, W., Downward movement of the soil moisture traced by means of hydrogen isotopes. In *Isotope Techniques in the Hydrologic Cycle*, Geophysical Monograph Series 11, American Geophysical Union, 1967.
11. Forstel, H., $^{18}\text{O}/^{16}\text{O}$ ratio of water in plants and their environment. In *Stable Isotopes* (eds Schmidt, H. L., Forstel, H. and Heinzinger, K.), Elsevier, Amsterdam, The Netherlands, 1982, pp. 503–516.
12. Irrigation Commission, *Irrigation Atlas of India*, National Atlas Organization, Kolkata, 1972.

Received 24 March 2003; revised accepted 15 September 2003